PHYSICAL REVIEW E **86**, 021914 (2012)

Excitation energy transfer modulated by oscillating electronic coupling of a dimeric system embedded in a molecular environment

Yosuke Suzuki[*]
Graduate School of Human Development and Environment, Kobe University, 3-11 Tsurukabuto, Nada, Kobe 657-8501, Japan

Shigenori Tanaka[†]
Graduate School of System Informatics, Kobe University, 1-1 Rokkodai, Nada, Kobe 657-8501, Japan

(Received 11 April 2012; revised manuscript received 7 June 2012; published 14 August 2012)

We have developed a theoretical formulation for excitation energy transfer between structurally fluctuating dimer molecules in surrounding environments. On the basis of a generalized master equation in which a memory function plays a vital role, the temporal evolutions of the population densities of exciton at the donor and acceptor sites are described. By employing an ansatz form for the memory function, the competitive effects of dimeric coupling and bath modes are analyzed quantitatively, where the roles of oscillating electronic coupling are highlighted.

DOI: 10.1103/PhysRevE.86.021914 PACS number(s): 87.15.R−, 82.20.−w, 71.35.−y, 05.40.−a

I. INTRODUCTION

Excitation energy transfer in biological and other molecular systems [1,2] has attracted much interest for a long time, and it still provides a field of hot debates experimentally and theoretically in various research subjects. For example, in the light-harvesting pigment-protein complexes in the neighborhood of photosynthetic reaction center, the excitation energy due to the light absorbed by pigments is transferred with extremely high efficiency. Recent experiments [3,4] have then suggested that long-lived quantum coherence in the exciton transfer plays an essential role for this high efficiency in the Fenna-Matthews-Olson (FMO) protein complex [5] of the green-sulfur bacterium *Chlorobium tepidum* and in the reaction center of the purple bacterium *Hodobacter sphaeroides*.

A lot of model calculations [1,2,6] have been carried out for elucidating the unique mechanism of the excitation energy transfer in photosynthetic systems. Of key interests in recent theoretical approaches [7–13] are the role of quantum coherence in the biological function of the chromophoric complexes and its competition or cooperation with the environmental relaxation effect due to the pigment-protein interactions in achieving the directed exciton flow. The roles played by the electronic coupling between the pigments and by the exciton-phonon coupling have thus been investigated by many researchers, yielding a wealth of insights into the sophisticated mechanism of efficient energy transfer realized in natural photosynthetic systems.

In this work, we especially focus on a physical effect which has been ignored in most of the theoretical analyses to date, but may play an important part in the description of the excitation energy transfer in biological and other molecular contexts. In many biomolecular systems, proteins or nucleic acids have a huge number of vibrational modes, which are localized or delocalized, and often show a large-scale cooperative motion. From a theoretical point of view, this effect can be incorporated into the model in terms of the electron-phonon or exciton-phonon coupling [1,2,14–16]. The shift or fluctuation of the site energies of excitons and the relaxation of excitation populations or coherences are described through these modelings, and additionally some inhomogeneities [2] in the site energies can be taken into account with model parameters as well. As compared with many attempts to account for these phonon-related effects, however, those effects that directly influence the strength of the electronic coupling between the excited pigments have rarely been incorporated in most model calculations. Since the electronic coupling is very sensitive to the distance and relative orientation of donor and acceptor, its value would be significantly affected by the structural modulations of molecular environments. It may be remarked in this context that the fluctuations in the electronic coupling between donor and acceptor have recently attracted much attention in the studies of electron transfer reactions in biological systems. It has been pointed out by many investigators [17–26] that those fluctuations in electronic coupling associated with the structural fluctuations of biomolecules may substantially modify the rate constant of pertinent electron transfer, thus having a biological significance. In addition, the effect of intermolecular torsional motion of π-aggregated dimer on excitation energy transfer has also been analyzed [27]. The purpose of this work is thus to theoretically investigate the effects of the correlated fluctuations of the electronic coupling between excitons on the temporal evolution of excitation energy transfer due to the conformational oscillations in molecular systems. In a preceding paper [28], a simple ansatz memory function to take account of the oscillation effect was employed in the generalized master equation (GME) for exciton transfer, which allowed for an analytic solution to the GME via a cubic algebraic equation. This work then proceeds to a more general, flexible form of the memory function, reflecting more reality.

In the following sections, a model which describes a single excitation transfer between a pair of symmetric pigments (homodimer) is considered, in which the exciton-phonon

---

[*] suzuki@radix.h.kobe-u.ac.jp
[†] tanaka2@kobe-u.ac.jp

coupling and the variation of the electronic coupling are taken into account. The model of homodimer is, of course, too simple to describe those complicated energy transfer phenomena as observed in the FMO complex, where multiple chromophores are involved [5,29]. However, the detailed investigations of this simple model would provide useful insights into mathematical structures underlying more complex systems. We consider the GME for the density matrix for describing the temporal evolution of the population densities of excitations at donor and acceptor. An ansatz form for the memory kernel associated with the temporal correlation function of the electronic coupling is then derived from model calculations and employed in the GME in order to include both the effects of the stochastic relaxation and the conformational oscillation due to the environmental phonons or bath modes. The consequent integrodifferential equation for the excitation energy transfer is solved as analytically as possible. The significance of the oscillatory modifications of the electronic coupling is then illustrated through model calculations for a wide variety of parameter sets.

II. THEORY

A. Generalized master equation (GME)

In this study, we consider the excitation energy transfer between donor (D) and acceptor (A) sites embedded in biomolecular or other environments. The Hamiltonian for the dimer system is given by [1]

$$H = H_0 + V, \tag{1}$$

where

$$H_0 = H_D|D\rangle\langle D| + H_A|A\rangle\langle A| \tag{2}$$

is the diagonal part in the site representation and

$$V = J\,(|A\rangle\langle D| + |D\rangle\langle A|) \tag{3}$$

represents the off-diagonal part [30,31]. In Eq. (2), H_D and H_A include both the contributions of the electronic excitation energies and the nuclear vibrations (phonons or bath modes) coupled with $|D\rangle$ and $|A\rangle$, respectively. Thus, the electron-phonon coupling that may modify the electronic energies and dynamics is taken into account implicitly in the following analysis. Let us consider the situation that the molecular environment surrounding the dimer system has a large number of vibrational modes, which may be described in terms of the normal mode analysis or the principal component analysis of the system [32,33]. We then assume that the electronic coupling J in Eq. (3) can be affected by these vibrational modes, which may be associated with the large-scale conformational oscillations [24,25,27]. Hereafter, for simplicity, we focus on the case of symmetric homodimer in which the donor and the acceptor have identical ground and excited states.

The system dynamics is described by the Liouville–von Neumann equation [1,15] as

$$i\hbar\frac{d\rho(t)}{dt} = [H,\rho(t)]\,. \tag{4}$$

The density matrix $\rho(t)$ is then expressed as

$$\rho(t) = \exp\left(-\frac{i}{\hbar}Ht\right)\rho(0)\exp\left(\frac{i}{\hbar}Ht\right), \tag{5}$$

where the initial condition at $t = 0$ is chosen so that the donor is in the excited state:

$$\rho(0) = |D\rangle\rho_b\langle D|. \tag{6}$$

In Eq. (6), ρ_b means the density matrix for the bath (phonon) subsystem, which may be assumed to be in the equilibrium state for H_D at $t = 0$.

Employing the interaction representations [1,15] as

$$\rho_I(t) = \exp\left(\frac{i}{\hbar}H_0t\right)\rho(t)\exp\left(-\frac{i}{\hbar}H_0t\right) \tag{7}$$

and

$$V_I(t) = \exp\left(\frac{i}{\hbar}H_0t\right)V\exp\left(-\frac{i}{\hbar}H_0t\right), \tag{8}$$

Eq. (4) is rewritten as

$$i\hbar\frac{d\rho_I(t)}{dt} = [V_I(t),\rho_I(t)] \equiv L_I(t)\rho_I(t), \tag{9}$$

where the Liouville operator $L_I(t)$ has been introduced. Here, we rely on the projection operator technique [34] and introduce a projection operator $\mathcal{P}$ which extracts the diagonal part of any operator in the site representation of the H_0 eigenstates; a complementary projection operator $\mathcal{Q}$, which selects the off-diagonal part, is also defined as $\mathcal{Q} = 1 - \mathcal{P}$. According to the procedure detailed in the preceding work [28,35–38], we then find

$$\frac{d}{dt}[\mathcal{P}\rho_I(t)] = -\frac{1}{\hbar^2}\int_0^t dt_1\mathcal{P}L_I(t)\mathcal{Q}L_I(t_1)\mathcal{P}\rho_I(t_1). \tag{10}$$

Here, we consider an explicit matrix representation for the diagonal part of the density matrix as

$$\mathcal{P}\rho_I(t) = \begin{pmatrix} \rho_D(t) & 0 \\ 0 & \rho_A(t) \end{pmatrix}, \tag{11}$$

and that for the electronic coupling

$$V_I(t) = \begin{pmatrix} V_{DD}(t) & V_{DA}(t) \\ V_{AD}(t) & V_{AA}(t) \end{pmatrix}. \tag{12}$$

After short algebra, we obtain a set of coupled equations for $\rho_D(t)$ and $\rho_A(t)$:

$$\frac{d}{dt}\rho_D(t) = -\frac{1}{\hbar^2}\int_0^t dt_1K(t,t_1)[\rho_D(t_1) - \rho_A(t_1)], \tag{13}$$

$$\frac{d}{dt}\rho_A(t) = -\frac{1}{\hbar^2}\int_0^t dt_1K(t,t_1)[\rho_A(t_1) - \rho_D(t_1)] \tag{14}$$

with

$$K(t,t_1) = V_{DA}(t)V_{AD}(t_1) + V_{AD}(t)V_{DA}(t_1). \tag{15}$$

The population densities of D and A are then given by

$$P_D(t) = \mathrm{Tr}_b\rho_D(t) \tag{16}$$

and

$$P_A(t) = \mathrm{Tr}_b\rho_A(t), \tag{17}$$

respectively, where Tr_b represents the trace over the vibrational states. Introducing a memory function by

$$M(t,t_1) = \frac{1}{\hbar^2}\langle K(t,t_1)\rangle_b = \frac{1}{\hbar^2}\mathrm{Tr}_b[\rho_b K(t,t_1)], \tag{18}$$

we finally obtain coupled master equations for $P_D(t)$ and $P_A(t)$ as

$$\frac{d}{dt}P_D(t) = \int_0^t dt_1[-M(t,t_1)P_D(t_1) + M(t,t_1)P_A(t_1)], \tag{19}$$

$$\frac{d}{dt}P_A(t) = \int_0^t dt_1[M(t,t_1)P_D(t_1) - M(t,t_1)P_A(t_1)]. \tag{20}$$

Since the population densities of D and A satisfy a relation

$$P_D(t) + P_A(t) = 1, \tag{21}$$

we may introduce a function

$$F(t) \equiv 1 - 2P_A(t), \tag{22}$$

which represents the population densities as

$$P_A(t) = \tfrac{1}{2}[1 - F(t)] \tag{23}$$

and

$$P_D(t) = \tfrac{1}{2}[1 + F(t)]. \tag{24}$$

Equations (19) and (20) are then reduced to

$$\frac{d}{dt}F(t) = -2\int_0^t dt_1 M(t,t_1)F(t_1), \tag{25}$$

where the memory function is given by

$$M(t,t_1) = \frac{1}{\hbar^2}\mathrm{Tr}_b\{\rho_b[V_{DA}(t)V_{AD}(t_1) + V_{AD}(t)V_{DA}(t_1)]\}. \tag{26}$$

The projection operator formalism developed above is related to another well-known formalism based on the phonon correlation functions, the detailed descriptions of which are found in the literature [1].

B. Memory function

The evaluation of the memory function, Eq. (26), derived above asks for the calculations of electronic coupling constant [31] for many conformations of molecular system that evolve temporally and generate a statistical ensemble at a temperature. Although it may be possible to numerically perform these calculations in an *ab initio* manner even for biomolecular systems by the combination of molecular dynamics and fragment molecular orbital methods [39–41], we assume an ansatz form

$$M(t,t_1) = \frac{2J_0^2}{\hbar^2}\exp\left(-\frac{t-t_1}{\tau_0}\right)\frac{1+\Delta\cos[\omega_0(t-t_1)]}{1+\Delta} \tag{27}$$

in the following analysis. Here, the parameters J_0, τ_0, ω_0, and Δ, which are assumed to be positive, characterize the strength of electronic coupling, the relaxation time, the oscillation frequency, and the magnitude of oscillation, respectively. It is noted that the relaxation time τ_0 describes the modification of electronic dynamics due to the electron-phonon coupling [38].

The oscillating factor in this memory function can be rationalized as follows. We first assume a short-range form [30,31] of electronic coupling as proportional to $\exp(-\beta x)$, where x is the distance between donor and acceptor, and β is a constant representing the spatial decay of the electronic coupling. Considering a vibrational behavior with a center x_0 and an amplitude Δx,

$$x = x_0 + \Delta x\cos\omega_0 t, \tag{28}$$

we express the time-dependent electronic coupling as

$$V(t) = V_0\mathrm{e}^{-\beta\Delta x\cos\omega_0 t}. \tag{29}$$

We then find

$$V(t)V(t+\tau) = V_0^2 e^{-\beta\Delta x[\cos\omega_0 t+\cos\omega_0(t+\tau)]}. \tag{30}$$

By performing the temporal averaging over the oscillation period, we obtain

$$\langle V(t)V(t+\tau)\rangle_t = \frac{\omega_0}{2\pi}\int_0^{\frac{2\pi}{\omega_0}} dt\, V_0^2 e^{-\beta\Delta x[\cos\omega_0 t+\cos\omega_0(t+\tau)]} = \frac{V_0^2}{\pi}\int_0^{\pi} d\theta\, e^{-z\cos\theta}, \tag{31}$$

where $\theta = \omega_0 t$ and $z = 2\beta\Delta x\cos\frac{\omega_0\tau}{2}$. We can rewrite this expression using the modified Bessel function $I_0(z)$ as

$$\langle V(t)V(t+\tau)\rangle_t = V_0^2 I_0(z) = V_0^2 I_0\left(2\beta\Delta x\cos\frac{\omega_0\tau}{2}\right). \tag{32}$$

Noting [42]

$$I_0(z) = \sum_{n=0}^{\infty}\frac{(z/2)^{2n}}{n!\Gamma(n+1)} = 1 + \frac{1}{4}z^2 + \dots, \tag{33}$$

and assuming $\beta\Delta x \ll 1$, Eq. (32) leads to

$$\langle V(t)V(t+\tau)\rangle_t \approx V_0^2\left[1 + \tfrac{1}{2}(\beta\Delta x)^2 + \tfrac{1}{2}(\beta\Delta x)^2\cos\omega_0\tau\right]. \tag{34}$$

We thus find an oscillating form

$$\langle V(t)V(t_1)\rangle \propto \frac{1+\Delta\cos[\omega_0(t-t_1)]}{1+\Delta}. \tag{35}$$

Further, we next consider another (long-range) case of $V \propto (x_1/x)^n$, where x_1 and n are constants. $V(t)$ may then be expressed as

$$V(t) = V_0\left(\frac{1}{1+\frac{\Delta x}{x_0}\cos\omega_0 t}\right)^n \tag{36}$$

according to Eq. (28), and hence

$$V(t)V(t+\tau)=V_0^2\left\{\frac{1}{1+\frac{2\Delta x}{x_0}\cos\left(\omega_0 t+\frac{\omega_0\tau}{2}\right)\cos\frac{\omega_0\tau}{2}+\frac{1}{2}\left(\frac{\Delta x}{x_0}\right)^2[\cos(2\omega_0 t+\omega_0\tau)+\cos\omega_0\tau]}\right\}^n. \tag{37}$$

Assuming $\frac{\Delta x}{x_0}\ll 1$, we find

$$\begin{aligned}\langle V(t)V(t+\tau)\rangle_t &\approx \frac{\omega_0 V_0^2}{2\pi}\int_0^{2\pi/\omega_0} dt\left\{1-2n\frac{\Delta x}{x_0}\cos\left(\omega_0 t+\frac{\omega_0\tau}{2}\right)\cos\frac{\omega_0\tau}{2}-\frac{n}{2}\left(\frac{\Delta x}{x_0}\right)^2[\cos(2\omega_0 t+\omega_0\tau)+\cos\omega_0\tau]\right.\\ &\quad\left.+2n(n+1)\left(\frac{\Delta x}{x_0}\right)^2\cos^2\left(\omega_0 t+\frac{\omega_0\tau}{2}\right)\cos^2\left(\frac{\omega_0\tau}{2}\right)\right\}\\ &= V_0^2\left[1+\frac{n(n+1)}{2}\left(\frac{\Delta x}{x_0}\right)^2+\frac{n^2}{2}\left(\frac{\Delta x}{x_0}\right)^2\cos\omega_0\tau\right].\end{aligned} \tag{38}$$

Therefore, $\langle V(t)V(t_1)\rangle$ is again expressed as Eq. (35). Finally, it is also remarked that the functional form of $\cos\omega_0(t-t_1)$ may arise from a different cause associated with an energy difference between two electronic states [35]. Thus, in what follows we will use the form of Eq. (35) without being restricted to the small Δ case.

C. Analytic solutions to GME

The integrodifferential equaiton we need to solve is Eq. (25) with Eq. (27). $P_A(t)$ and $P_D(t)$ can then be calculated from $F(t)$ immediately. We can solve this integrodifferential equation by using the Laplace transform technique [42]. With the initial condition of $F(0)=1$, the solution is written as follows:

$$F(t)=\frac{1}{2\pi i}\int_{\sigma-i\infty}^{\sigma+i\infty} ds\, e^{st}\left[s+\frac{4J_0^2}{\hbar^2(1+\Delta)}\left(\frac{1}{s+\frac{1}{\tau_0}}+\frac{\Delta\left(s+\frac{1}{\tau_0}\right)}{\left(s+\frac{1}{\tau_0}\right)^2+\omega_0^2}\right)\right]^{-1}, \tag{39}$$

where σ is chosen so that all the singular points of the integrand lie to the left of the line Re$s=\sigma$ in the complex s plane. Thus, if the solutions to the quartic equation

$$s^4+\frac{3}{\tau_0}s^3+\left(\frac{3}{\tau_0^2}+\omega_0^2+\frac{4J_0^2}{\hbar^2}\right)s^2+\left(\frac{1}{\tau_0^3}+\frac{\omega_0^2}{\tau_0}+\frac{8J_0^2}{\hbar^2}\frac{1}{\tau_0}\right)s+\frac{4J_0^2}{\hbar^2}\left(\frac{1}{\tau_0^2}+\frac{\omega_0^2}{1+\Delta}\right)=0 \tag{40}$$

are expressed by $s=\alpha,\beta,\gamma,\delta$, we obtain

$$\begin{aligned}F(t)&=\frac{(\alpha+1/\tau_0)\left[(\alpha+1/\tau_0)^2+\omega_0^2\right]}{(\alpha-\beta)(\alpha-\gamma)(\alpha-\delta)}e^{\alpha t}+\frac{(\beta+1/\tau_0)\left[(\beta+1/\tau_0)^2+\omega_0^2\right]}{(\beta-\alpha)(\beta-\gamma)(\beta-\delta)}e^{\beta t}\\ &\quad+\frac{(\gamma+1/\tau_0)\left[(\gamma+1/\tau_0)^2+\omega_0^2\right]}{(\gamma-\alpha)(\gamma-\beta)(\gamma-\delta)}e^{\gamma t}+\frac{(\delta+1/\tau_0)\left[(\delta+1/\tau_0)^2+\omega_0^2\right]}{(\delta-\alpha)(\delta-\beta)(\delta-\gamma)}e^{\delta t}.\end{aligned} \tag{41}$$

Before considering the case of finite value of Δ, we study some limiting cases for which already known results would be recovered. When Δ goes to infinity, Eq. (40) becomes

$$\left(s+\frac{1}{\tau_0}\right)\left[s^3+\frac{2}{\tau_0}s^2+\left(\frac{1}{\tau_0^2}+\omega_0^2+\frac{4J_0^2}{\hbar^2}\right)s+\frac{4\hbar^2}{\hbar^2}\frac{1}{\tau_0}\right]=0. \tag{42}$$

The solution to this equation can be expressed by $-\frac{1}{\tau_0}$, $\tilde{\alpha}$, $\tilde{\beta}$, and $\tilde{\gamma}$. Equation (41) then becomes

$$\begin{aligned}F(t)&=\frac{(\tilde{\alpha}+1/\tau_0)^2+\omega_0^2}{(\tilde{\alpha}-\tilde{\beta})(\tilde{\alpha}-\tilde{\gamma})}e^{\tilde{\alpha}t}+\frac{(\tilde{\beta}+1/\tau_0)^2+\omega_0^2}{(\tilde{\beta}-\tilde{\alpha})(\tilde{\beta}-\tilde{\gamma})}e^{\tilde{\beta}t}\\ &\quad+\frac{(\tilde{\gamma}+1/\tau_0)^2+\omega_0^2}{(\tilde{\gamma}-\tilde{\alpha})(\tilde{\gamma}-\tilde{\beta})}e^{\tilde{\gamma}t},\end{aligned} \tag{43}$$

which agrees with the one already obtained [28].

If $\Delta\to 0$, Eq. (40) becomes

$$\left(s^2+\frac{1}{\tau_0}s+\frac{4J_0^2}{\hbar^2}\right)\left[\left(s+\frac{1}{\tau_0}\right)^2+\omega_0^2\right]=0. \tag{44}$$

We thus find

$$\begin{aligned}F(t)&=\frac{1}{2}\left(\frac{1}{\tau_0\sqrt{D}}+1\right)e^{(-\frac{1}{2\tau_0}+\sqrt{D/4})t}\\ &\quad-\frac{1}{2}\left(\frac{1}{\tau_0\sqrt{D}}-1\right)e^{(-\frac{1}{2\tau_0}-\sqrt{D/4})t},\end{aligned} \tag{45}$$

where $D=\frac{1}{\tau_0^2}-\frac{16J_0^2}{\hbar^2}$ [28].

Next we consider general cases. Introducing parameters $a=\frac{1}{\tau_0^2}$, $b=\omega_0^2$, $c=\frac{4J_0^2}{\hbar^2}$, and $d=\Delta$, Eq. (40) becomes

$$s^4+3\sqrt{a}s^3+(3a+b+c)s^2+\sqrt{a}(a+b+2c)s+c\left(a+\frac{b}{1+d}\right)=0, \tag{46}$$

and we hereafter denote the left-hand side of this equation by $f(s)$. The solutions to Eq. (46) are expressed as

$$\begin{aligned}
\alpha &= -\frac{3\sqrt{a}}{4} + \frac{\sqrt{t_1}+\sqrt{t_2}+\sqrt{t_3}}{2},\\
\beta &= -\frac{3\sqrt{a}}{4} + \frac{\sqrt{t_1}-\sqrt{t_2}-\sqrt{t_3}}{2},\\
\gamma &= -\frac{3\sqrt{a}}{4} + \frac{-\sqrt{t_1}+\sqrt{t_2}-\sqrt{t_3}}{2},\\
\delta &= -\frac{3\sqrt{a}}{4} + \frac{-\sqrt{t_1}-\sqrt{t_2}+\sqrt{t_3}}{2},
\end{aligned} \tag{47}$$

where t_1, t_2, and t_3 are the solutions to the following cubic equation:

$$t^3 + k_2 t^2 + k_1 t + k_0 = 0, \tag{48}$$

where

$$\begin{aligned}
k_2 &= -\frac{3}{4}a + 2b + 2c,\\
k_1 &= -[(3a-8b-8c)^2 - 4(3a^2 + 3a^2 d + 48ab\\
&\quad + 48abd - 16ac - 16acd - 256bc)]/[16384(1+d)],\\
k_0 &= -\frac{a}{64}(a+4b-4c)^2,
\end{aligned} \tag{49}$$

with $\sqrt{t_1}\sqrt{t_2}\sqrt{t_3} = -\frac{\sqrt{a}}{8}(a+4b-4c)$ being satisfied. One then finds

$$\begin{aligned}
t_1 &= \tfrac{1}{6}\{-2k_2 + [4(V_1 + 3\sqrt{W_1})]^{\frac{1}{3}}\\
&\quad + [4(V_1 - 3\sqrt{W_1})]^{\frac{1}{3}}\},\\
t_2 &= \tfrac{1}{6}\{-2k_2 + \omega[4(V_1 + 3\sqrt{W_1})]^{\frac{1}{3}}\\
&\quad + \omega^2[4(V_1 - 3\sqrt{W_1})]^{\frac{1}{3}}\},\\
t_3 &= \tfrac{1}{6}\{-2k_2 + \omega^2[4(V_1 + 3\sqrt{W_1})]^{\frac{1}{3}}\\
&\quad + \omega[4(V_1 - 3\sqrt{W_1})]^{\frac{1}{3}}\},
\end{aligned} \tag{50}$$

where

$$\begin{aligned}
V_1 &= -27k_0 + 9k_2k_1 - 2k_2^3,\\
W_1 &= 3\big(27k_0^2 - 18k_2k_1k_0 + 4k_1^3 + 4k_2^3k_0 - k_2^2k_1^2\big),\\
\omega &= \frac{-1+\sqrt{3}i}{2},
\end{aligned} \tag{51}$$

and the products of any two roots should be $4(k_2^2 - 3k_1)$.

Here, we derive the conditon that α, β, γ, and δ are real numbers all together. The discriminant of the quartic equation (46) is

$$\begin{aligned}
D_4 = 256C_0^3 &- \big(27C_3^4 + 192C_3C_1 - 144C_3^2C_2 + 128C_2^2\big)C_0^2\\
&- \big(6C_3^2C_1^2 + 4C_3^2C_2^3 + 80C_3C_2^2C_1 - 144C_2C_1^2\\
&- 16C_2^4 - 18C_3^3C_2C_1\big)C_0 - \big(4C_3^3C_1 - 18C_3C_2C_1\\
&- C_3^2C_2^2 + 27C_1^2 + 4C_2^3\big)C_1^2,
\end{aligned} \tag{52}$$

where

$$\begin{aligned}
C_3 &= 3\sqrt{a},\\
C_2 &= 3a + b + c,\\
C_1 &= \sqrt{a}(a + b + 2c),\\
C_0 &= c[a + b/(1+d)].
\end{aligned} \tag{53}$$

The derivative of the left-hand side of Eq. (46) is

$$\begin{aligned}
f'(s) &= 4s^3 + 9\sqrt{a}s^2 + 2(3a+b+c)s\\
&\quad + \sqrt{a}(a+b+2c).
\end{aligned} \tag{54}$$

The discriminant of the cubic equation $f'(s) = 0$ is then

$$\begin{aligned}
D_3 &= -108a^2b + 36ab^2 + 504abc + 36ac^2 - 128b^3\\
&\quad - 384b^2c - 384bc^2 - 128c^3.
\end{aligned} \tag{55}$$

If $D_3 > 0$, $f(s)$ has three (real) minimal or maximal points; α', β', and γ', which are the solutions to $f'(s) = 0$, are then expressed by

$$\begin{aligned}
\alpha' &= -\tfrac{3}{4}\sqrt{a} + \tfrac{1}{12}[(V_2 + 12\sqrt{W_2})^{\frac{1}{3}} + (V_2 - 12\sqrt{W_2})^{\frac{1}{3}}],\\
\beta' &= -\tfrac{3}{4}\sqrt{a} + \tfrac{1}{12}[\omega(V_2 + 12\sqrt{W_2})^{\frac{1}{3}} + \omega^2(V_2 - 12\sqrt{W_2})^{\frac{1}{3}}],\\
\gamma' &= -\tfrac{3}{4}\sqrt{a} + \tfrac{1}{12}[\omega^2(V_2 + 12\sqrt{W_2})^{\frac{1}{3}} + \omega(V_2 - 12\sqrt{W_2})^{\frac{1}{3}}],
\end{aligned} \tag{56}$$

where

$$\begin{aligned}
V_2 &= 27\sqrt{a}(a + 4b - 4c),\\
W_2 &= 27a^2b - 9ab^2 - 126abc - 9ac^2 + 96b^2c\\
&\quad + 96bc^2 + 32b^3 + 32c^3,
\end{aligned} \tag{57}$$

with the products of any two roots being $9a - 24b - 24c$.

If $D_4 > 0$, the solutions to $f(s) = 0$ are either all real numbers or all complex numbers with imaginary parts. If α', β', γ' are real and $f[\min(\alpha',\beta',\gamma')] < 0$ or $f[\max(\alpha',\beta',\gamma')] < 0$, two of the solutions are real at least. Therefore, the condition that all the solutions to $f(s) = 0$ are real is $D_4 > 0$, $D_3 > 0$, and $f[\min(\alpha',\beta',\gamma')] < 0$ or $f[\max(\alpha',\beta',\gamma')] < 0$. Using another expression, the condition is $D_3 > 0$, $f[\min(\alpha',\beta',\gamma')] < 0$, $f[\mathrm{median}(\alpha',\beta',\gamma')] > 0$ and $f[\max(\alpha',\beta',\gamma')] < 0$, which is equivalent to the above one. On the other hand, when the equation $f(s) = 0$ has at least two complex solutions with imaginary parts, $F(t)$ may exhibit an oscillatory behavior associated with the quantum coherence of exciton energy transfer (*vide infra*).

III. NUMERICAL RESULTS AND DISCUSSION

In the following analyses, for simplicity, we employ a value of $\tau_0 = 100$ fs. We adopted this value according to a case for FMO protein [9,29], while this specification is made only for the sake of numerical illustrations since only the relative amplitudes among the model parameters are essential (see Fig. 4 below). We first show in Fig. 1 the temporal variations of $P_A(t)$, where J_0 and ω_0 are varied in the range of 10 fs $\leqslant \hbar/J_0, \omega_0^{-1} \leqslant$ 1000 fs, and Δ is set equal to be unity. For a fixed value of ω_0, an oscillatory behavior of $P_A(t)$ appears with the increase of the coupling strength J_0, which is associated with the quantum coherence of exciton transfer. The

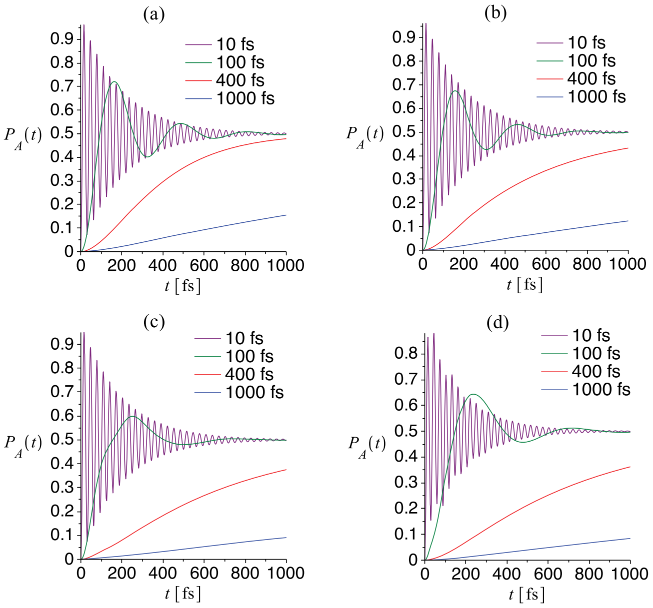

FIG. 1. (Color) Temporal evolutions of the population density of exciton at the acceptor site $P_A(t)$ for $\tau_0 = 100$ fs, $\Delta = 1$, and $\hbar/J_0 =$ 1000 (blue), 400 (red), 100 (green), 10 (purple) fs. (a) $\omega_0^{-1} = 1000$ fs. (b) $\omega_0^{-1} = 100$ fs. (c) $\omega_0^{-1} = 30$ fs. (d) $\omega_0^{-1} = 10$ fs.

structural oscillation represented by ω_0 and Δ then modulates this behavior of $P_A(t)$ through the interference with the effect of J_0. As seen in Fig. 1, this effect modifies the frequency of oscillation in $P_A(t)$ as well as its magnitude. Figure 2 then illustrates the details in the case of $\omega_0^{-1} = 30$ fs for 100 fs $\leqslant \hbar/J_0 \leqslant$ 400 fs. It is noted that the oscillation in $P_A(t)$ does not always appear even when the quartic equation (46) has solutions with imaginary part. Although Eq. (46) has two real and two complex roots for $\hbar/J_0 > 286$ fs, the oscillation is not observed. $P_A(t)$ has both the oscillating and damping components, and the oscillation does not appear when the overdamping terms dominate $P_A(t)$. On the other hand, Eq. (46) has four complex roots for $\hbar/J_0 < 286$ fs, and the oscillation is observed.

Figure 3 shows the results of $P_A(t)$ for $\hbar/J_0 = 100$ fs and 8 fs $\leqslant \omega_0^{-1} \leqslant$ 800 fs, where the quartic equation (46) has four solutions, all of which have imaginary parts. It is interesting that the variation of $P_A(t)$ as a function of ω_0^{-1} is not monotonous; the amplitude of oscillation is significantly suppressed in the case of $\omega_0^{-1} = 40$ fs. This is due to the effect of interference between two oscillating modes with different frequencies and similar magnitudes.

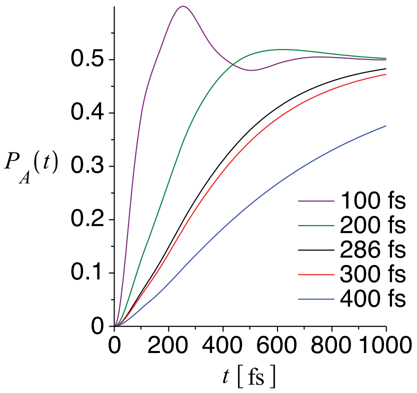

FIG. 2. (Color) Temporal evolutions of the population density of exciton at the acceptor site $P_A(t)$ for $\tau_0 = 100$ fs, $\omega_0^{-1} = 30$ fs, $\Delta =$ 1, and $\hbar/J_0 = 400$ (blue), 300 (red), 286(black), 200 (green), 100 (purple) fs.

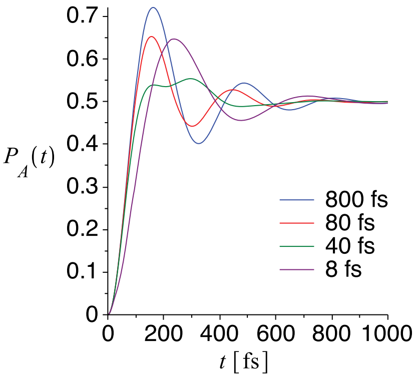

FIG. 3. (Color) Temporal evolutions of the population density of exciton at the acceptor site $P_A(t)$ for $\tau_0 = 100$ fs, $\Delta = 1$, $\hbar/J_0 =$ 100 fs, and $\omega_0^{-1} = 800$ (blue), 80 (red), 40 (green), 8 (purple) fs.

Phase diagrams for the behavior of $P_A(t)$ are illustrated in Fig. 4 for various values of Δ. The solutions to the quartic

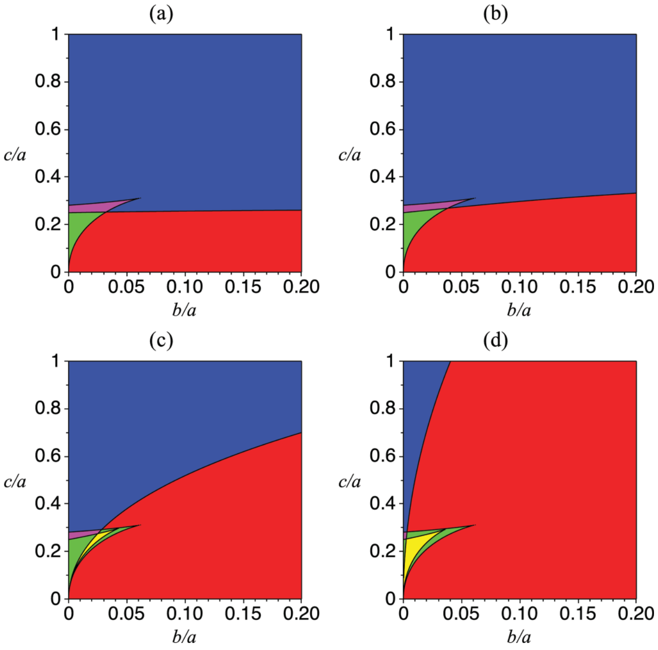

FIG. 4. (Color) Phase diagrams for the behavior of the population density $P_A(t)$ as a function of b/a and c/a. (i) Blue region: superposition of two oscillating contributions with $D_4 > 0$ and $D_3 < 0$; Eq. (46) has four complex roots. (ii) Purple: superposition of two oscillating contributions with $D_4 > 0$ and $D_3 > 0$ (four complex roots). (iii) Green: superposition of one damped oscillation term and two monotonously decaying terms with $D_4 < 0$ and $D_3 > 0$ (two real and two complex roots). (iv) Red: superposition of one damped oscillation term and two monotonously decaying terms with $D_4 < 0$ and $D_3 < 0$ (two real and two complex roots). (v) Yellow: superposition of four decaying terms with $D_4 > 0$ and $D_3 > 0$ (four real roots). (a) $\Delta = 0.1$. (b) $\Delta = 1$. (c) $\Delta = 10$. (d) $\Delta = 100$.

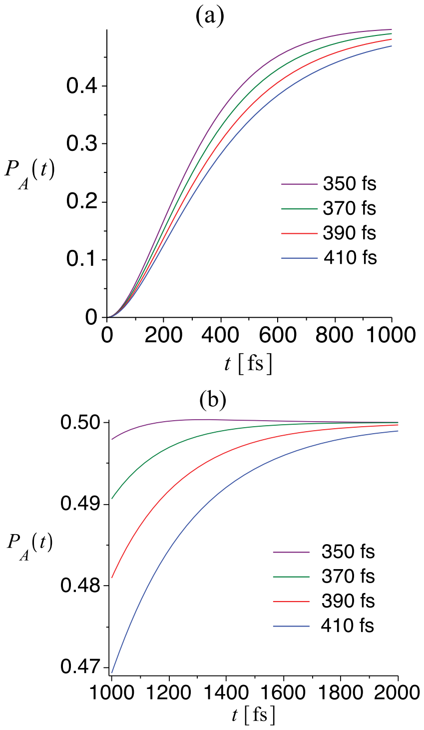

FIG. 5. (Color) Temporal evolutions of the population density of exciton at the acceptor site $P_A(t)$ for $\tau_0 = 100$ fs, $\omega_0^{-1} = 580$ fs, $\Delta = 10$, and $\hbar/J_0 = 410$ fs [blue: the equation of $f(s) = 0$ has two real and two complex solutions], 390 fs (red: four real solutions), 370 fs (green: two real and two complex solutions), 350 fs (purple: four complex solutions). (a) 0 fs $\leqslant t \leqslant$ 1000 fs. (b) 1000 fs $\leqslant t \leqslant$ 2000 fs.

equation (46) may have imaginary parts or not, which is depicted by the color representation over the b/a versus c/a plane. The parameter region in which all the four solutions are real, represented by yellow color in Fig. 4, appears in the cases of $\Delta = 10$ and 100. In some parts of the red and green regions, the oscillation in $P_A(t)$ is not observed due to the overdamping effect. In the blue and purple regions, where $P_A(t)$ does not have the overdamping terms, the oscillation of $P_A(t)$ is observed.

Figure 5 shows the calculated results of $P_A(t)$ for $\tau_0 = 100$ fs, $\omega_0^{-1} = 580$ fs, and $\Delta = 10$. With the increase of J_0, the number of solutions to the quartic equation (46) with imaginary parts varies. Only in the case of $\hbar/J_0 = 350$ fs, where all the four solutions have imaginary parts, is the oscillatory behavior of $P_A(t)$ visible in the figure. In the case of $\hbar/J_0 = 390$ fs, the equation has four real roots, and $P_A(t)$ does not show the oscillation. In the cases of $\hbar/J_0 = 410$ and 370 fs, the quartic equation has two real and two complex roots, whereas a difference exists between them. In the latter case, $P_A(t)$ is observed to have a maximum at $t \approx 2525$ fs (not shown), while in the former case $P_A(t)$ is a monotonously increasing function of time. This is because the damping effects work differently. In the case of $\hbar/J_0 = 370$ fs, the simple damping terms have shorter time scales than the damped oscillation term. After the damping terms have become hardly effective, the oscillation term becomes a major contribution to $P_A(t)$.

When the equation $f(s) = 0$ has four solutions with imaginary part, $P_A(t)$ can be expressed as

$$P_A(t) = 0.5 + \sum_{i=1}^{2} h_i(t), \tag{58}$$

where $h_i(t) = A_i \exp(-t/\tau_i)\cos(\omega_i t + \phi_i)$. We here introduce an index to represent the contribution arising from the minor oscillation part

$$I = \frac{\min\left\{\int_0^\infty [h_1(t)]^2\, dt, \int_0^\infty [h_2(t)]^2\, dt\right\}}{\sum_{i=1}^{2}\int_0^\infty [h_i(t)]^2\, dt}, \tag{59}$$

which takes a value between 0 and 0.5. The behavior of $P_A(t)$ can then be described in terms of a single $h_i(t)$ function if I vanishes, otherwise $P_A(t)$ would be expressed as a superposition of two damped oscillating functions. Let us then observe the cases of $\hbar/J_0 = 10$ fs in Figs. 1(c) and 1(d), where $I = 1.2 \times 10^{-3}$ and 1.5×10^{-2} for the former and the latter, respectively. This analysis thus explains that the former shows a simple damped oscillating behavior, while the amplitude of the latter does not always decay as a function of time. Further, we find $I = 3.1 \times 10^{-6}$, 5.7×10^{-2}, 0.14, 6.0×10^{-5} for $\omega_0^{-1} = 800$, 80, 40, and 8 fs in Fig. 3. Therefore, one observes simple damped oscillations in the cases of $\omega_0^{-1} = 800$ and 8 fs. On the other hand, the superposition effect of oscillations is visible in the cases of $\omega_0^{-1} = 80$ and 40 fs, which is especially significant in the latter case.

IV. CONCLUSION

On the basis of the generalized master equation, we have proposed a theoretical formulation to describe the excitation energy transfer between dimeric molecules. Environmental effects arising from surroundings are taken into account in terms of memory function which can be evaluated as a temporal correlation function of electronic coupling between donor and acceptor. In particular, an oscillation effect that was overlooked in earlier studies has been highlighted in this work. Assuming an ansatz form for the memory function, we can quantitatively discuss the effects of dimeric coupling, relaxation, and oscillation due to phonon modes on the exciton dynamics. Conversely, it would be possible to extract the information about the molecular parameters from the behavior of exciton transfer observed in experiments. The present theory thus provides a basis for these analyses, which would be useful for explaining experimental results accumulated in photosynthetic and other research fields such as those for molecular aggregates [27,43].

---

[1] V. May and O. Kuhn, *Charge and Energy Transfer Dynamics in Molecular Systems* (Wiley-VCH, Berlin, 2011).

[2] T. Renger, V. May, and O. Kuhn, Phys. Rep. **343**, 138 (2001).

[3] G. S. Engel, T. R. Calhoun, E. L. Read, T.-K. Ahn, T. Mancal, Y.-C. Cheng, R. E. Blankenship, and G. R. Fleming, Nature (London) **446**, 782 (2007).

[4] H. Lee, Y.-C. Cheng, and G. R. Fleming, Science **316**, 1462 (2007).
[5] J. M. Olson, Photosynth. Res. **80**, 181 (2004).
[6] A. Ishizaki, T. R. Calhoun, G. S. Schlau-Cohen, and G. R. Fleming, Phys. Chem. Chem. Phys. **12**, 7319 (2010).
[7] S. Jang, Y.-C. Cheng, D. R. Reichman, and J. D. Eaves, J. Chem. Phys. **129**, 101104 (2008).
[8] M. Mohseni, P. Rebentrost, S. Lloyd, and A. Aspuru-Guzik, J. Chem. Phys. **129**, 174106 (2008).
[9] A. Ishizaki and G. R. Fleming, Proc. Natl. Acad. Sci. USA **106**, 17255 (2009).
[10] F. Caruso, A. W. Chin, A. Datta, S. F. Huelga, and M. B. Plenio, J. Chem. Phys. **131**, 105106 (2009).
[11] J. Cao and R. J. Silbey, J. Phys. Chem. A **113**, 13825 (2009).
[12] G. D. Scholes, J. Phys. Chem. Lett. **1**, 2 (2010).
[13] A. Kelly and Y. M. Rhee, J. Phys. Chem. Lett. **2**, 808 (2011).
[14] V. M. Agranovich and M. D. Galanin, *Electronic Excitation Energy Transfer in Condensed Matter* (North-Holland, Amsterdam, 1982).
[15] S. Mukamel, *Principles of Nonlinear Optical Spectroscopy* (Oxford University Press, New York, 1995).
[16] T. Renger and R. A. Marcus, J. Chem. Phys. **116**, 9997 (2002).
[17] I. Daizadeh, E. S. Medvedev, and A. A. Stuchebrukhov, Proc. Natl. Acad. Sci. USA **94**, 3703 (1997).
[18] J. Antony, D. M. Medvedev, and A. A. Stuchebrukhov, J. Am. Chem. Soc. **122**, 1057 (2000).
[19] A. Troisi and G. Orlandi, J. Phys. Chem. B **106**, 2093 (2002).
[20] J. Creechley and Y. Dahnovsky, Chem. Phys. **296**, 171 (2004).
[21] Y. Dahnovsky, Phys. Rev. B **73**, 144303 (2006).
[22] H. Nishioka, A. Kimura, T. Yamato, T. Kawatsu, and T. Kakitani, J. Phys. Chem. B **109**, 15621 (2005).
[23] T. Kubar, P. B. Woiczikowski, G. Cuniberti, and M. Elstner, J. Phys. Chem. B **112**, 7937 (2008).
[24] D. Hennig, E. B. Starikov, J. F. R. Archilla, and F. Palmero, J. Biol. Phys. **30**, 227 (2004).
[25] E. B. Starikov, Philos. Mag. **85**, 3435 (2005).
[26] S. Tanaka and E. B. Starikov, Phys. Rev. E **81**, 027101 (2010).
[27] J. Seibt and A. Eisfeld, J. Chem. Phys. **136**, 024109 (2012).
[28] S. Tanaka, Chem. Phys. Lett. **508**, 139 (2011).
[29] J. Adolphs and T. Renger, Biophys. J. **91**, 2778 (2006).
[30] M. D. Newton, Chem. Rev. **91**, 767 (1991).
[31] C.-P. Hsu, Acc. Chem. Res. **42**, 509 (2009).
[32] Q. Cui and I. Bahar, *Normal Mode Analysis* (Chapman & Hall/CRC, Boca Raton, 2006).
[33] S. Tanaka, Phys. Lett. A **372**, 1280 (2008).
[34] R. Zwanzig, Physica (Amsterdam) **30**, 1109 (1964).
[35] V. M. Kenkre and R. S. Knox, Phys. Rev. B **9**, 5279 (1974).
[36] A. Kimura and T. Kakitani, J. Phys. Chem. B **107**, 14486 (2003).
[37] A. Kimura and T. Kakitani, J. Phys. Chem. A **111**, 12042 (2007).
[38] A. Kimura, T. Kakitani, and T. Yamato, J. Phys. Chem. B **104**, 9276 (2000).
[39] M. Ito, K. Fukuzawa, T. Ishikawa, Y. Mochizuki, T. Nakano, and S. Tanaka, J. Phys. Chem. B **112**, 12081 (2008).
[40] K. Takematsu, K. Fukuzawa, K. Omagari, S. Nakajima, K. Nakajima, Y. Mochizuki, T. Nakano, H. Watanabe, and S. Tanaka, J. Phys. Chem. B **113**, 4991 (2009).
[41] A. Tagami, N. Ishibashi, D. Kato, N. Taguchi, Y. Mochizuki, H. Watanabe, M. Ito, and S. Tanaka, Chem. Phys. Lett. **472**, 118 (2009).
[42] M. R. Spiegel, *Mathematical Handbook of Formulas and Tables* (McGraw-Hill, New York, 1968).
[43] A. Gelzinis, D. Abramavicius, and L. Valkunas, Phys. Rev. B **84**, 245430 (2011).